Available online at www.sciencedirect.com

ScienceDirect

journal homepage: www.elsevier.com/locate/watres

The effect of dichlorophen binding to silica nanoparticles on its photosensitized degradation in water

Juan P. Escalada [a], Valeria B. Arce [b], Gabriela V. Porcal [c], M. Alicia Biasutti [c], Susana Criado [c], Norman A. García [c], Daniel O. Mártire [b,*]

[a] Unidad Académica Río Gallegos de la Universidad Nacional de la Patagonia Austral, Argentina
[b] Instituto de Investigaciones Fisicoquímicas Teóricas y Aplicadas (INIFTA), CCT-La Plata-CONICET, Universidad Nacional de La Plata, Diag 113 y 64, La Plata, Argentina
[c] Departamento de Química, Universidad Nacional de Río Cuarto, Campus Universitario, Río Cuarto, Argentina

ARTICLE INFO

Article history:
Received 8 August 2013
Received in revised form
29 November 2013
Accepted 2 December 2013
Available online 12 December 2013

Keywords:
Dichlorophen
Photodegradation
Silica nanoparticles
Natural waters

ABSTRACT

The production of dichlorophen (2,2′-methylenebis(4-chlorophenol), DCP) and its use as an anthelmintic and in pesticide products result in its direct release to the environment. To the purpose of modelling the possible photodegradation routes of DCP sorbed on sediments or suspended particles, the synthesis and characterization of silica nanoparticles modified with DCP (NP–DCP) is reported.

The reactivity of NP–DCP with the excited states of riboflavin, a sensitizer usually present in natural waters, and with singlet oxygen were investigated. Comparison of the kinetic results obtained here to those previously reported for irradiated aqueous solutions of DCP allowed the discussion of the effect of adsorption of the pesticide on its photodegradation.

We show with the aid of computer simulations that in natural waters the relevance of the different photodegradation routes dichlorophen is very much affected by attachment to sediments.

1. Introduction

The production of dichlorophen (2,2′-methylenebis(4-chlorophenol), DCP) and its use as an anthelmintic and in pesticide products result in its direct release to the environment. DCP has been recognized as very toxic to aquatic organisms and may cause long-term effects in the aquatic environment (EC Directive 2001/58/EC). Once released to the environment, its hydrophobicity allows it to bioconcentrate in marine organisms, bioaccumulate, and eventually biomagnify. Previous studies have reported that DCP can be accumulated in fish exposed to wastewater treatment works effluents and this compound was also detected in wastewater effluents at concentrations of 10–450 ngL^{-1}, a fact which indicates that its presence is mainly due to its widespread use also as a bactericide and fungicide in a variety personal care product formulations (Hill et al., 2010; Rostkowski et al., 2011).

The degradation of a pesticide in an aquatic natural environment can be carried out by direct photolysis or through its

* *Corresponding author*. Tel.: +54 221 425 7430; fax: +54 221 425 4642.
E-mail addresses: dmartire@inifta.unlp.edu.ar, danielmartire@gmail.com (D.O. Mártire).

0043-1354/$ – see front matter © 2013 Elsevier Ltd. All rights reserved.
http://dx.doi.org/10.1016/j.watres.2013.12.006

reaction with reactive oxygen species (ROS) if another light-absorbing compound – a photosensitizer – is present in the medium. Among the sensitizers usually present in water courses, lakes and seas are humic acids (HA) (Carlos et al., 2011) and the pigment riboflavin (Rf) (Escalada et al., 2006).

Based on the estimated Koc value it can be predicted that if released to water, DCP adsorbs strongly to suspended solids and sediment in the water column (Toxicology Data Network). The adsorption of dissolved DCP to suspended silica particles in natural waters motivated us to synthesize silica nanoparticles functionalized with DCP (NP–DCP) by employing the condensation reaction 1.

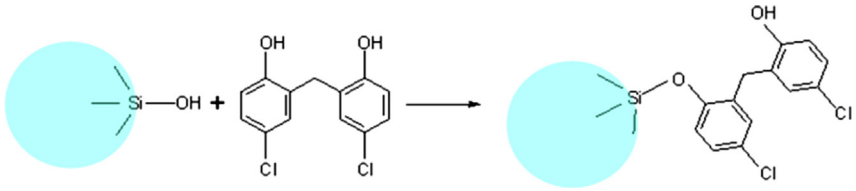

(1)

Note that reaction 1 depicts the anchoring of DCP to the silica nanoparticles but does not mean the existence of only one bonded molecule of DCP per nanoparticle.

The photodegradation of DCP mediated by Rf, a sensitizer usually present along with HA in water courses, lakes and seas (Escalada et al., 2006; Zeng et al., 2003; Benassi et al., 1967), was recently investigated (Escalada et al., 2011). Upon visible light irradiation and in the absence of interacting compounds, the contribution of HA to the generation of reactive oxygen species (ROS) is very small, if compared to that of Rf (Carlos et al., 2011; Leech et al., 2009). For this reason, the sensitizer Rf was recently employed as proxy of chromophore dissolved organic matter (DOM) (Vione et al., 2011).

With this background we set out to investigate the kinetics of the possible routes leading to the photosensitized degradation of the silica particles modified with DCP suspended in aqueous solutions of Rf. Comparison of the kinetic results obtained here to those previously reported for irradiated aqueous solutions of the phenolic pesticide (Escalada et al., 2011) allows the discussion of the effect of adsorption of the pesticide on its photodegradation.

2. Materials and methods

2.1. Reagents

Fumed silica (Sigma, specific surface area; SSA = (390 ± 40) m^2/g, particle diameter estimated from the SSA = 7 nm) was dried in a crucible for 15 h at 120 °C and then in a muffle for 3 h at 250 °C and stored in desiccators. The solvent *o*-xylene (Aldrich) was distilled onto molecular sieves, which had been dried at 250 °C for 4 h. Superoxide dismutase (SOD), DCP, furfuryl alcohol (FFA), deuterium oxide (D_2O), deuterated methanol (MeOD) and $CaCl_2$, all from Sigma–Aldrich, rose bengal (RB) and sodium azide from Anedra, CaH_2 (Fluka), 2-propanol and methanol (MeOH) from Sintorgan, ethyl acetate (Ciccarelli, p.a.), and K_2HPO_4 and KH_2PO_4 (Merck) were used without further purification.

2.2. Synthesis of the nanoparticles

A modification of the condensation method reported for the synthesis of nanoparticles functionalized with alcohols (Ruiz et al., 2007; Arce et al., 2011) was employed here (see reaction 1). Briefly, 0.5 g of DCP and 180 mL of *o*-xylene were added to 1.0 g of silica nanoparticles. The mixtures were placed in a Soxhlet extractor containing CaH_2 equipped with a condenser with anhydrous $CaCl_2$, and refluxed during 24 h. The products were filtered with 20 nm- nylon filters, washed with 50 mL hot *o*-xylene and finally with 50 mL ethyl acetate. The resulting gel was first dried at 0.1 Torr and at room temperature for 3 h and then at 120 °C for 5 h. White powders were obtained.

To reduce colloidal aggregation the aqueous suspensions of NP–DCP were buffered with a mixture of K_2HPO_4 and KH_2PO_4 (pH = 6.4) (Ruiz et al., 2007).

2.3. Characterization of the nanoparticles

The particles were characterized by Fourier transform infrared spectroscopy (FTIR), Brunauer-Emmett-Teller (BET) analysis, thermogravimetry (TG), dynamic light scattering (DLS), and UV–vis spectroscopy. The experimental details are given in the Supplementary data.

2.4. Fluorescence spectroscopy

Fluorescence lifetimes were evaluated with a time-correlated single photon counting technique (SPC) on an Edinburgh FL-9000CD instrument provided with a PicoQuant subnanosecond pulsed LED emitting at 450 nm. The emission wavelength for Rf was 515 nm. The measurements were performed with solutions of Rf ($A^{450} = 0.23$) in aqueous phosphate buffer of pH = 6.4 and with (0–2.5 gL^{-1}) NP–DCP suspensions in this solution.

Steady state fluorescence anisotropy measurements $< r >$ were obtained from eq. (2) using a Hitachi 2500 spectrofluorometer.

$$< r >= \frac{I_{VV} - GI_{VH}}{I_{VV} + 2GI_{VH}} \quad (2)$$

(2)where I_{VV} and I_{VH} are the vertically and horizontally polarized emission components after excitation by vertically polarized light and G is the sensitivity factor of the detection system.

All measurements were carried out at 25 °C.

2.5. Laser flash-photolysis (LFP) experiments

LFP experiments were performed by excitation with the third harmonic (355 nm) of a Nd:YAG (Spectron SL 400) laser (18 ns fwhm). The analysis light from a 150 W Xe arc lamp was passed through a PTI monochromator and detected by a R666 Hamamatsu photomultiplier coupled to a HP54504 digital oscilloscope. For the electronically excited Rf triplet states (^{3}Rf*) quenching experiments Ar-saturated buffered aqueous or unbuffered methanol NP–DCP suspensions in Rf solutions were employed.

2.6. Quenching of singlet molecular oxygen, $O_2(^1\Delta_g)$, experiments

To measure the overall quenching rate constant of $O_2(^1\Delta_g)$, k_t, buffered D_2O or unbuffered MeOD solutions of RB ($A^{532} = 0.33$) were employed. NP–DCP were suspended in the solutions. Laser irradiation of the air-saturated samples at 532 nm with *ca.* 18 ns pulse width was carried out with a Nd:YAG laser (Spectron Laser SL 400). The detection and acquisition systems are described elsewhere (Criado et al., 1997). The signals from 10 laser pulses were averaged and the obtained signals were fitted to a monoexponential function of time, characterized by τ_Δ, the singlet oxygen lifetime.

The rate constant k_r for the chemical reaction of $O_2(^1\Delta_g)$ with NP–DCP was measured by comparative continuous irradiation experiments performed in aqueous medium, according to a described method (Tratniek and Hoigné, 1991). The sensitizer employed was RB and the irradiation was carried out in a home-made photolyser with filtered light (>350 nm, cut-off filter) from a 150-W quartz halogen lamp. Under these conditions, the pseudo first-order slope for the consumption of oxygen is proportional to k_r. The ratio of these slopes to those obtained in comparative experiments under identical experimental conditions but with a reference substrate for which k_r is known (FFA is used here, ($k_r = 1.2 \times 10^8\ M^{-1}\ s^{-1}$ (Tratniek and Hoigné, 1991)), allows the determination of k_r for the sample. The oxygen concentration was measured with an oxygen-sensitive electrode (Orion 97-0899).

2.7. Measurement of the quantum yield of direct photolysis of DCP and NP–DCP

Two different excitation sources were employed: the 254 nm light from a 15 W- Platinum low pressure mercury lamp and the 307.6 nm output from a zinc hollow cathode lamp passed through a 300 nm cut-off filter. The incident photon rate (P_0), measured using potassium ferrioxalate as actinometer (Carlos et al., 2012a) were 1.12×10^{-6} and 7.95×10^{-9} E s^{-1} L^{-1} at 254 and 307.6 nm, respectively.

The quantum yield of direct photolysis (Φ) of DCP and NP–DCP were measured.

Quantification of DCP was performed by HPLC using a Shimadzu CMB-20A instrument, as described in the Supplementary data.

The optical density spectra of the NP–DCP suspensions were modelled as the sum of a scattering component ($a + c/\lambda^n$) fit and an absorption component according to Ruiz et al. (2007). The scattering component, obtained from a least-squares minimization from 400 to 700 nm, was extrapolated at lower wavelengths. The absorption contribution was calculated by subtracting the scattering component from the measured optical density. Quantification of DCP bonded to NP–DCP was done by measurement of the absorption component obtained from UV–visible spectroscopy. In order to minimize the interference of photoproducts, very short irradiation times ($t < 3$ min) were employed. However, as this procedure might not guarantee the complete elimination of the possible interference of the photoproducts, an upper limit of the quantum yield is obtained.

3. Results

3.1. Characterization of NP–DCP

The TG of the NP–DCP shows three distinct stages (see Figure S1 in the Supplementary data). The first one from room temperature to 200 °C corresponds to the elimination of the remaining washing solvents. The second step from 200 to 650 °C is related to the organic moiety bonded to silica (de Farias and Airoldi, 1998) and the last stage from 650 to 800 °C corresponds to the remaining silanol condensation, to give the siloxane units (Sales et al., 2006). The percentage of organic groups (%OG, w/ w) calculated from the thermogravimetry is 5%.

From DLS measurements, two populations of average hydrodynamic diameters of NP–DCP were determined (Table 1). These results are indicative of the aggregation of the 7 nm-diameter modified nanoparticles.

3.2. Quantum yields of direct photolysis (Φ)

The values of Φ for DCP measured at $\lambda^{exc} = 254$ nm following substrate consumption after irradiation in the absence and presence of oxygen are 0.13 ± 0.02 and 0.14 ± 0.02, respectively. Consumption of DCP bonded to the particles monitored by UV–visible spectroscopy yielded $\Phi \leq 0.14 \pm 0.02$ for irradiation of air-saturated suspensions. Experiments performed with air-saturated DCP solutions at $\lambda^{exc} = 307.6$ nm yielded 0.13 ± 0.03, which shows that the quantum yield of DCP photolysis is independent of the excitation wavelength in the range 254–307.6 nm.

Table 1 – Results of NP–DCP characterization.

Technique	Parameter	
DLS	Hydrodynamic diameter (nm) and full width at half maxima (FWHM)	173 (231) 1610 (1041)
BET	S_{BET} ($m^2\ g^{-1}$)	160.7 ± 0.6
TG	%OG (w/w)	5%

3.3. *Kinetics of the interaction of reactive oxygen species with NP–DCP*

The discussion of the results will be based on Scheme 1. This scheme is similar to that employed for interpreting the interaction between Rf excited states and $O_2(^1\Delta_g)$ and DCP in solution (Escalada et al., 2011).

3.3.1. *Fluorescence experiments*

The fluorescence lifetime of Rf in suspensions of the NP–DCP or of the bare silica nanoparticles ($\tau_F = 4.9$ ns) was independent of the concentration of suspended particles in the concentration range 0–2.5 gL^{-1} (26 μM). This observation means that under these conditions the concentration of surface groups of the modified particles is too small to affect the fluorescence lifetime of Rf, which is in line with the low content of organic groups of the NP–DCP (Table 1). For this reason, the rate constant of reaction (3) (^1k_q) could not be measured.

The fluorescence anisotropy $<r> = 0.005$ measured for the solutions of Rf in the aqueous phosphate buffer were coincident with those measured with the 2.5 gL^{-1} suspensions of NP–DCP in the same solvent. This result indicates that Rf is not adsorbed on the NP–DCP, at least in freshly prepared solutions. Thus, Scheme 1 considers that the sensitizer is dissolved in solution.

3.3.2. *Laser flash-photolysis (LFP)*

The absorbance of ^{3}Rf* was monitored at 670 nm, a zone where the overlapping with other possible species is negligible. The triplet decay was measured at low Rf concentration (typical 0.02 mM) and at low enough laser energy, to avoid self-quenching and triplet–triplet annihilation. The decay of ^{3}Rf* was fitted to single exponential functions both in Ar-saturated aqueous or methanol solutions of the sensitizer.

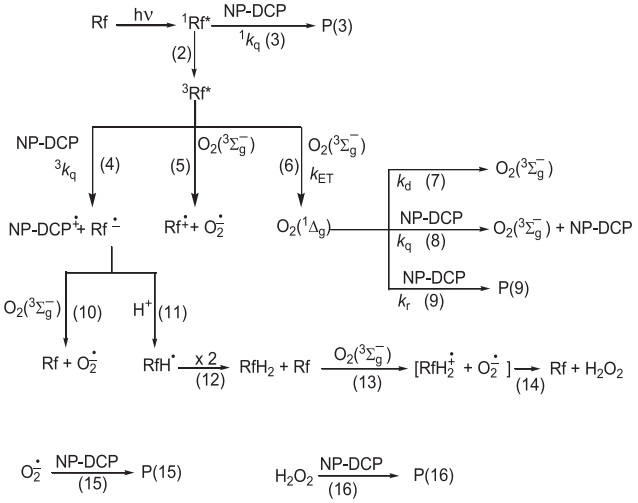

Scheme 1 – Main processes taking place upon visible-light irradiation of Rf in the presence of NP–DCP. P(3), P(9), P(15), and P(16) are reaction products. $O_2(^3\Sigma_g^-)$ stands for ground state oxygen. The overall quenching constant of $O_2(^1\Delta_g)$ by NP–DCP k_t is the sum of the rate constants k_q and k_r, processes (8) and (9), respectively.

The decays of ^{3}Rf* in 3.1 gL^{-1} (1.3×10^{-5} M) suspensions of the bare SiO_2 in Ar-saturated water or methanol suspensions were coincident with those measured in the neat solvents. This result means that any reaction of ^{3}Rf* with the silanol groups of the particles can be neglected.

The decay rate of ^{3}Rf* in buffered water or unbuffered methanol samples increased with increasing concentration of suspended NP–DCP, as can be seen in Fig. 1 for the aqueous suspensions (inset). Taking the mass of one NP–DCP approximately equal to that of one bare SiO_2 nanoparticle (3.95×10^{-19} g) (Arce et al., 2011), the bimolecular rate constants ^3k_q for the quenching of ^{3}Rf* by the particles (per mole of NP–DCP) in suspensions calculated from the linear plots of τ_T^{-1} vs. [NP–DCP] are $(3.30 \pm 0.08) \times 10^{10}$ and $(3.4 \pm 0.3) \times 10^{10}$ M^{-1} s^{-1}, respectively (see Fig. 1 for the data in aqueous medium). From the 5% OG w/w obtained from the TG analysis, ^3k_q can also be expressed per mole of DCP (Table 2).

In order to further explore the type of interaction between ^{3}Rf* and NP–DCP, transient absorption spectra were recorded. Fig. 2 shows the spectrum obtained here 2 μs after the laser pulse in aqueous solution, which was assigned to the T–T absorption spectrum of ^{3}Rf* (Escalada et al., 2011). In the presence of 1 gL^{-1} NP–DCP, where 90% of the triplet states of ^{3}Rf* are quenched by the organic groups of NP–DCP, the transient spectrum taken 20 μs after the laser pulse is coincident with that of the semiquinone radical, RfH$^{\bullet}$ (Lu et al., 2004) formed from the radical anion Rf$^{\bullet-}$ (processes (4) and (11) in Scheme 1). As for the quenching of ^{3}Rf* by DCP in solution (Escalada et al., 2011), in this case it was not possible either to observe the absorption of any oxidized product of DCP.

3.3.3. *Continuous irradiation experiments in the presence of selective scavengers of ROS*

To obtain further information on the reactive species involved in the Rf-photosensitized degradation of NP–DCP, the concentration of dissolved oxygen was measured upon continuous irradiation of NP–DCP suspensions in Rf solutions. The photoirradiation ($\lambda = 470 \pm 30$ nm) of a suspension of NP–DCP (0.5 gL^{-1}) in Rf (0.023 mM) solution gave rise to oxygen consumption. The participation of ROS was evaluated through oxygen consumption experiments in the presence of specific

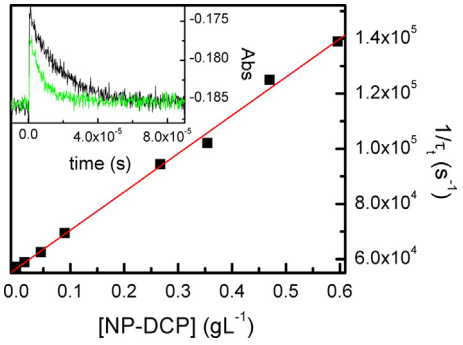

Fig. 1 – Plot of the reciprocal of the triplet lifetime vs. [NP–DCP]. Inset: Decay of ^{3}Rf* (λ = 670 nm) in Ar-saturated aqueous phosphate buffer in the absence (upper signal) and presence of 0.09 gL^{-1} (middle signal), and 0.47 gL^{-1} (lower signal) NP–DCP.

Table 2 – Quenching rate constants of $^3Rf^*$ and $O_2(^1\Delta_g)$ by NP–DCP and DCP.

Solvent	Quencher	^3k_q (M^{-1} s^{-1})	k_t (M^{-1} s^{-1})	k_r (M^{-1} s^{-1})
H_2O or D_2O	NP–DCP	$(7.5 \pm 0.18) \times 10^8$ [a,b]	$(1.1 \pm 0.1) \times 10^8$ [a,b]	$(8.6 \pm 0.5) \times 10^8$ [a,b]
	DCP	____ [c]	$(2.70 \pm 0.05) \times 10^8$ [d]	$(8.7 \pm 0.4) \times 10^7$ [d]
MeOH or MeOD	NP–DCP	$(7.6 \pm 0.7) \times 10^8$ [a,b]	$(9.6 \pm 0.5) \times 10^7$ [b]	$(1.0 \pm 0.1) \times 10^8$ [a,b]
	DCP	$(2.1 \pm 0.1) \times 10^9$ [d]	$(8.0 \pm 0.1) \times 10^6$ [d]	$(2.0 \pm 0.2) \times 10^6$ [d]

[a] From this work.
[b] Expressed per mole of DCP.
[c] Not measured due to the low solubility of DCP in H_2O.
[d] From ref. Escalada et al., 2011.

scavengers (inset of Fig. 3). The decrease of oxygen consumption in the presence of NaN_3 (10 mM) and SOD (1 μg/mL) confirm the participation of $O_2(^1\Delta_g)$ and $O_2^{\bullet-}$ respectively. In the presence of NaN_3 the steady-state concentration of $O_2(^1\Delta_g)$ decreases and thus, the rate of reaction (9) responsible for oxygen consumption diminishes. The effect of SOD is explained through dismutation of $O_2^{\bullet-}$, which makes reaction (14) less favourable. The addition of 2-Propanol (20 mM), within the experimental error, had a minor effect (if any) on the rate of oxygen uptake. Thus, the participation of the hydroxyl radical can be considered negligible.

3.3.4. *Quenching of $O_2(^1\Delta_g)$ experiments*

To determine the overall quenching rate constant (k_t) of $O_2(^1\Delta_g)$ by NP–DCP in buffered D_2O (pD = 6.4), the decay of the time-resolved $O_2(^1\Delta_g)$ phosphorescence signal was measured by employing RB as the sensitizer (λ^{exc} = 532 nm). The decay rate of $O_2(^1\Delta_g)$ increases with increasing concentration of NP–DCP (Fig. 4 inset). The Stern-Volmer plot is shown in Fig 4. The bimolecular rate constant k_t expressed per mole of DCP is shown in Table 2.

4. Discussion

4.1. *Comparison of the rate constants for the reactions of DCP and NP–DCP with $^3Rf^*$ and $O_2(^1\Delta_g)$*

Table 2 also shows the rate constants for the reactions of $^3Rf^*$ and $O_2(^1\Delta_g)$ with DCP in solution for comparative purposes.

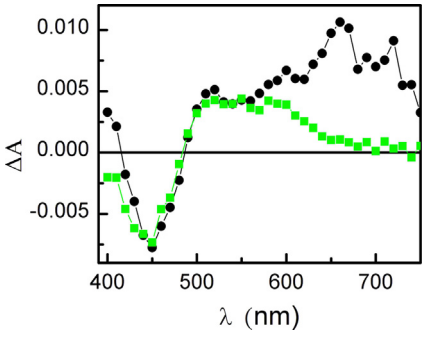

Fig. 2 – Transient absorption spectra of Rf (A^{355} = 0.2) in Ar-saturated aqueous phosphate buffer in the absence (circles) taken 2 μs after the laser pulse and in the presence of 1 gL^{-1} NP–DCP (squares) taken 20 μs after the laser pulse.

It can be seen in Table 2 that the reaction between $^3Rf^*$ and NP–DCP is diffusion-controlled, as observed for the reaction of other modified silica nanoparticles of the same size with benzophenone triplet states (Ruiz et al., 2007).

Table 2 also shows that in MeOH on a per mole of DCP basis, immobilization of DCP on the silica nanoparticles results in an almost 3-fold decrease of the reaction rate constant of the pesticide with $^3Rf^*$. A similar ratio is obtained between the rate constant k_t of the reaction of $O_2(^1\Delta_g)$ with DCP in solution and NP–DCP in aqueous D_2O.

However, in aqueous medium the decrease of the rate constant k_r is of one order of magnitude or larger when the DCP molecules are attached to the silica nanoparticles.

The values of k_t and k_r for NP–DCP expressed per mole of DCP measured in MeOH and MeOD, respectively, are higher than those reported for the free pesticide in the same solvents (see Table 2). A possible explanation to this fact is that adsorption of anionic RB is favoured in this solvent in comparison to H_2O or D_2O because of the negative surface charge of the nanoparticles in aqueous medium due to deprotonation of the silanol groups (Ong et al., 1992). Should an interfacial reaction between the newly generated $O_2(^1\Delta_g)$ by adsorbed RB and chemisorbed DCP occur, then a rate enhancement of the heterogeneous reaction would be expected (Demeter and Bérces, 1989).

All these results indicate that immobilization of the pesticide involving the phenolic group of DCP in the attachment to

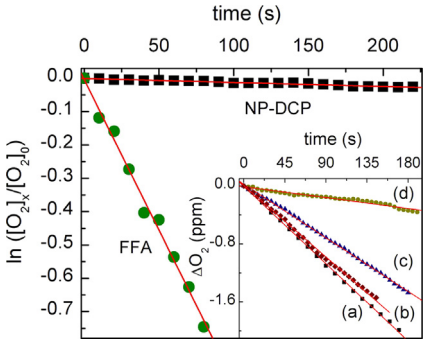

Fig. 3 – First order plots for oxygen uptake in buffered H_2O suspensions of 0.5 gL^{-1} NP–DCP and 0.5 mM solutions of FFA, as indicated. RB was used as sensitizer (A^{548} = 0.5). Inset: Oxygen consumption vs. photoirradiation time obtained from NP–DCP aqueous suspensions in Rf solutions in the absence (a) and presence of 20 mM 2-propanol (b), 1 μg/mL SOD (c), and 10 mM Na_3N (d).

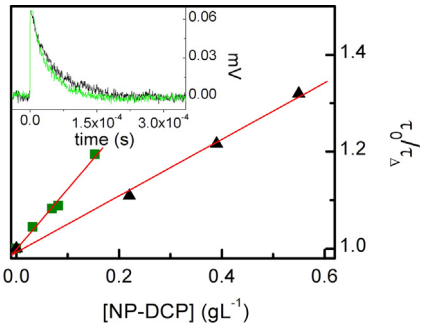

Fig. 4 – Plot of τ_0/τ_Δ vs. [NP–DCP] in D_2O (squares) and MeOD (triangles). Inset: Phosphorescence signal of decay of $O_2(^1\Delta_g)$ in air-saturated D_2O phosphate buffer (pD = 6.4) in the absence (upper signal) and 0.15 gL^{-1} (lower signal) NP–DCP.

the particles produces a decrease of the reactivity of DCP with excited ^{3}Rf* and $O_2(^1\Delta_g)$. Thus, at this point an evaluation of the environmental consequences of the chemical adsorption on this contaminant on sediments or suspended particles seems pertinent.

4.2. *Simulation of the photodegradation of DCP and NP–DCP in natural waters*

Natural reservoirs contain oxidizing species at low steady-state concentrations (see Table 3), such as excited triplet states of dissolved organic matter, ^{3}DOM*, $O_2(^1\Delta_g)$, and HO· radicals, which are able to oxidize DCP. Furthermore, DCP absorbs light and thus, the direct photolysis must also be considered. In order to evaluate the detoxifying capacity of natural waters towards DCP free or chemisorbed on silica, the minimal reaction mechanism shown in Table 3 was considered in computer simulations. In this mechanism the substrate S stands for dissolved or adsorbed DCP. DCP chemisorbed on DCP-NP was used to mimic DCP adsorbed on natural silica.

The rate constants of the reactions of $O_2(^1\Delta_g)$ with DCP and NP–DCP employed in the simulations are those shown in Table 2. Since Rf can be employed as proxy of chromophore DOM (Vione et al., 2011), for the rate constants between the substrates S and ^{3}DOM*, the values of the corresponding rate constants between ^{3}Rf* and S were used. Although Rf can be employed to simulate DOM in natural waters, we should consider that as in addition to Rf-like substances, other species with different photochemical properties are present in these media. For the reactions of S with hydroxyl radicals diffusion-controlled values of 3×10^{10} M^{-1} s^{-1} were employed (Smoluchowski, 1917).

The average half life $t_{1/2}$ of S can be obtained from eq. (3).

$$t_{1/2} = \ln 2 / \left(k_{17} \times [^3\mathrm{DOM}*]_{SS} + k_{18} \times [O_2(^1\Delta_g)]_{SS} + k_{19} \times [HO^\cdot]_{SS} + ka \times \Phi \right) \quad (3)$$

(3)where $[^3\mathrm{DOM}^*]_{ss}$, $[O_2(^1\Delta_g)]_{ss}$, and $[HO^\cdot]_{ss}$ represent the molar steady-state concentrations of the reactive species; k_a is the specific rate of light absorption and Φ is the photolysis quantum yield (0.13 for DCP and the upper limit of 0.14 for NP–DCP, see above). The reaction of DCP with carbonate radicals was not considered because of the low steady-state concentration of this species in natural waters (10^{-13}–10^{-15} M) (Dell'Arciprete et al., 2012) along with the low rate constant of the reactions of this radical with phenols (NDRL-NIST Solution Kinetics Database).

The calculation of k_a considering the reported underwater midday solar irradiance in the wavelength range from 300 to 320 nm (Zepp, 1978) and neglecting any screening of sunlight due to DOM (Carlos et al., 2012b) is shown in the Supplementary data. The quantum yields of DCP and NP–DCP photodegradation under air-saturation (see Section 3.2) led to a value of $t_{1/2}$ of 2.3 h for free DCP and a much longer one (7.3 h) for the more resistant to photodegradation chemisorbed pesticide.

The solution of the mass differential equations built for the set of reactions of the minimal mechanism considering the average steady-state concentrations of the reactive species shown in Table 3 and the calculated value of $k_a = 1.02 \times 10^{-4}$ s^{-1} yields information on the amount of S depleted due to the different reactive intermediates in natural waters. The simulated relative depletion of substrate S after 10 h of disposal in the natural water is shown in Fig. 5. At this time the depletion of DCP and NP–DCP are about 95 and 62%, respectively.

Table 3 – Reactions involved in the depletion of DCP in natural waters.

Reaction	Steady-state concentration of the oxidant species in natural waters/ M or the specific rate of light absorption of DCP beyond 300 nm, k_a.
S + ^{3}DOM* → P17 (17)	$[^3\mathrm{DOM}^*]_{ss} = 10^{-13}$–$10^{-15}$ [a]
S + $O_2(^1\Delta_g)$ → P18 (18)	$[O_2(^1\Delta_g)]_{ss} = 10^{-12}$-$10^{-13}$ [b]
S + HO· → P19 (19)	$[HO^\cdot]_{ss}$ = radicals 10^{-17}–10^{-15} [c]
S + hν → P20 (20)	$k_a = 1.02 \times 10^{-4}$ s^{-1}

[a] From Canonica et al. (1995).
[b] From Zepp and Cline (1977).
[c] From Vione et al. (2006).

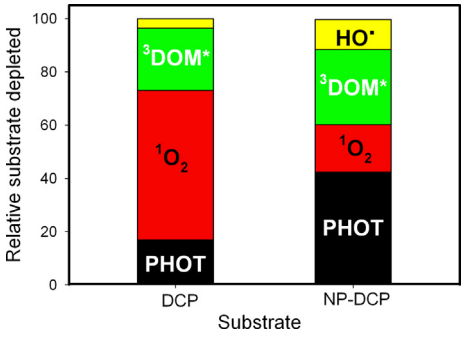

Fig. 5 – Simulated DCP and NP–DCP degradation after 10 h in natural waters. The consumption due to direct photolysis (PHOT), and to reactions with $O_2(^1\Delta_g)$, ^{3}DOM*, and HO· are shown from bottom to top.

As can be seen in Fig. 5 the less significant route of pesticide consumption is through reaction with $HO^{\cdot}$ radicals. Fig. 5 also shows that the main photochemical sinks of the free pesticide follow the trend $O_2(^1\Delta_g) > {}^3DOM^* >$ direct photolysis, while for the chemisorbed pesticide the tendency is direct photolysis$> {}^3DOM^* > O_2(^1\Delta_g)$. The observed change in the relative relevance of the different photodegradation routes is due to the lower reactivity of the chemisorbed pesticide with the reactive species (Table 2). The involvement of $^3DOM^*$ in the chemisorbed pesticide consumption becomes more important than of $O_2(^1\Delta_g)$ because of the drastic decrease of k_r upon adsorption on silica.

5. Conclusion

Dichlorophen bonded to silica nanoparticles reacts with the electronically excited triplet states of riboflavin by electron transfer, as also does the free pesticide, although with a lower rate constant. In aqueous medium the rates of both the overall and chemical deactivation of $O_2(^1\Delta_g)$ by the chemisorbed dichlorophen are also lower than those by the free pesticide. The decrease of k_r is drastic due to the involvement of the phenolic group of dichlorophen in the bonding to the silica particles. As a result, the simulations of photodegradation of dichlorophen in natural waters show that when bonded to particles the relative contribution of the $O_2(^1\Delta_g)$ route becomes less important than when the pesticide is free in solution.

Consideration of Riboflavin as proxy of chromophore DOM allowed us to show with the aid of computer simulations that in natural waters the relevance of the different photodegradation routes dichlorophen is very much affected by attachment to sediments or suspended particles.

Acknowledgement

This research was supported by ANPCyT, Argentina (PICT 2008 # 00686), and CIC (Buenos Aires, Argentina). J.P.E. thanks CONICET (Argentina) for a post-doctoral fellowship. G.V.P., M.A.B., S.C., and N.A.G. are research members of CONICET. V.B.A. and D.O.M. are research members of CIC. The authors thank Dr. C. Airoldi for the thermogravimetry measurement.

Appendix A. Supplementary data

Supplementary data related to this article can be found at http://dx.doi.org/10.1016/j.watres.2013.12.006.

REFERENCES

Arce, V.B., Bertolotti, S.G., Oliveira, F.J.V.E., Airoldi, C., Gonzalez, M.C., Allegretti, P.E., Mártire, D.O., 2011. Safranine-T triplet-state quenching by modified silica nanoparticles. J. Phys. Chem. C 115 (37), 18122–18130.

Benassi, C.A., Scoffone, E., Galiazzo, G., Jori, G., 1967. Proflavine-sensitized photooxidation of tryptophan and related peptides. Photochem. Photobiol. 28 (12), 857–862.

Canonica, S., Jans, U., Stemmler, K., Hoigne, J., 1995. Transformation kinetics of phenols in water: photosensitization by dissolved natural organic material and aromatic ketones. Environ. Sci. Technol. 29 (7), 1822–1831.

Carlos, L., Pedersen, B.W., Ogilby, P.R., Mártire, D.O., 2011. The role of humic acid aggregation on the kinetics of photosensitized singlet oxygen production and decay. Photochem. Photobiol. Sci. 10, 1080–1086.

Carlos, L., Cipollone, M., Soria, D.B., Moreno, S., Ogilby, P.R., García Einschlag, F.S., Mártire, D.O., 2012a. The effect of humic acid binding to magnetite nanoparticles on the photogeneration of reactive oxygen species. Sep. Purif. Technol. 91, 23–29.

Carlos, L., Mártire, D.O., Gonzalez, M.C., Gomis, J., Bernabeu, A., Amat, A.M., Arques, A., 2012b. Photochemical fate of a mixture of emerging pollutants in the presence of humic substances. Water Res. 46 (15), 4732–4740.

Criado, S., Bertolotti, S.G., Soltermann, A.T., García, N.A., 1997. Kinetics studies on the photosensitized oxidation ($O_2(^1\Delta_g)$-mediated) of tryptophan-alkyl esters in Triton X-100 micellar solutions. J. Photochem. Photobiol. B 38 (2–3), 107–113.

de Farias, R.F., Airoldi, C., 1998. Thermogravimetry as a reliable tool to estimate the density of silanols on a silica gel surface. J. Therm. Anal. 53 (3), 751–756.

Dell'Arciprete, M.L., Soler, J., Santos-Juanes, L., Arques, A., Mártire, D.O., Furlong, J., Gonzalez, M.C., 2012. Reactivity of neonicotinoid insecticides with carbonate radicals. Water Res. 46 (11), 3479–3489.

Demeter, A., Bérces, T., 1989. Study of the long-lived intermediate formed in the photoreduction of benzophenone by isopropyl alcohol. J. Photochem. Photobiol., A 46 (1), 27–40.

Escalada, J.P., Pajares, A., Gianotti, J., Biasutti, A., Criado, S., Molina, P., Massad, W., Amat-Guerri, F., Garcia, N.A., 2011. Photosensitized degradation in water of the phenolic pesticides bromoxynil and dichlorophen in the presence of riboflavin, as a model of their natural photodecomposition in the environment. J. Hazard. Mater. 186 (1), 466–472.

Escalada, J.P., Pajares, A., Gianotti, J., Massad, W.A., Bertolotti, S., Amat-Guerri, F., Garcia, N.A., 2006. Dye-sensitized photodegradation of the fungicide carbendazim and related benzimidazoles. Chemosphere 65 (2), 237–244.

Hill, E.M., Evans, K.L., Horwood, J., Rostkowski, P., Oladapo, F.O., Gibson, R., Shears, J.A., Tyler, C.R., 2010. Profiles and some initial identifications of (anti)androgenic compounds in fish exposed to wastewater treatment works effluents. Environ. Sci. Technol. 44 (3), 1137–1143.

Leech, D.M., Matthew, T., Snyder, R.G., Wetzel, R.W., 2009. Natural organic matter and sunlight accelerate the degradation of 17 β-estradiol in water. Sci. Total Environ. 407 (6), 2087–2209.

Lu, C., Bucher, G., Sander, W., 2004. Photoinduced interactions between oxidized and reduced lipoic acid and riboflavin (vitamin B2). Chem. Phys. Chem. 5 (1), 47–56.

NDRL-NIST Solution Kinetics Database. ©NIST, 2002. http://kinetics.nist.gov/solution/, (accessed 01.08.13.).

Ong, S., Zhao, X., Eisenthal, K.B., 1992. Polarization of water molecules at a charged interface: second harmonic studies of the silica/water interface. Chem. Phys. Lett. 191 (3–4), 327–335.

Rostkowski, P., Horwood, J., Shears, J.A., Lange, A., Oladapo, F.O., Besselink, H.T., Tyler, C.R., Hill, E.M., 2011. Bioassay- directed identification of novel antiandrogenic compounds in bile of fish exposed to wastewater effluents. Environ. Sci. Technol. 45 (24), 10660–10667.

Ruiz, A.E., Caregnato, P., Arce, V.B., Schiavoni, M.M., Mora, V.C., Gonzalez, M.C., Allegretti, P.E., Mártire, D.O., 2007. Synthesis

and characterization of butoxylated silica nanoparticles. Reaction with benzophenone triplet states. J. Phys. Chem. C 111 (21), 7623–7628.
Sales, J.A.A., Petrucelli, G.C., Oliveira, F.J.V.E., Airoldi, C., 2006. Some features associated with organosilane groups grafted by the sol-gel process onto synthetic talc-like phyllosilicate. J. Colloid Interf. Sci. 297 (1), 95–103.
Smoluchowski, M.V., 1917. Versuch einer mathematischen Theorie der Koagulationskinetik kolloider Lösungen. Z. Phys. Chem. 92, 129–168.
Toxicology Data Network, http://toxnet.nlm.nih.gov/, (accessed 27.05.13.).
Tratniek, P.G., Hoigné, J., 1991. Oxidation of substituted phenols in the environment:a QSAR analysis of rate constants for reaction with singlet oxygen. Environ. Sci. Technol. 25 (9), 1956–1964.
Vione, D., Falletti, G., Maurino, V., Minero, C., Pelizzetti, E., Malandrino, M., Ajassa, R., Olariu, R., Arsene, C., 2006. Sources and sinks of hydroxyl radicals upon irradiation of natural water samples. Environ. Sci. Technol. 40 (12), 3775–3781.
Vione, D., Maddigapu, P.R., De Laurentiis, E., Minella, M., Pazzi, M., Maurino, V., Minero, C., Kouras, S., Richard, C., 2011. Modelling the photochemical fate of ibuprofen in surface. Water Res. 45 (20), 6725–6736.
Zeng, K., Hwang, H., Zhang, Y., Yu, H., 2003. Identification of 6-aminochrysene photoproducts and study of the effect of a humic acid and riboflavin on its photolysis. J. Photochem. Photobiol. B: Biol. 72 (1–3), 95–100.
Zepp, R.G., Cline, D.M., 1977. Rates of direct photolysis in aquatic environment. Environ. Sci. Technol. 11 (4), 359–366.
Zepp, R.G., 1978. Quantum yields for reaction of pollutants in dilute aqueous solution. Environ. Sci. Technol. 12 (3), 327–329.